Bioimaging

DOI: 10.1002/ange.201408897

Mitochondria-Targeted Cancer Therapy Using a Light-Up Probe with Aggregation-Induced-Emission Characteristics**

*Qinglian Hu, Meng Gao, Guangxue Feng, and Bin Liu**

Abstract: *Subcellular organelle-specific reagents for simultaneous tumor targeting, imaging, and treatment are of enormous interest in cancer therapy. Herein, we present a mitochondria-targeting probe (AIE-mito-TPP) by conjugating a triphenylphosphine (TPP) with a fluorogen which can undergo aggregation-induced emission (AIE). Owing to the more negative mitochondrial membrane potential of cancer cells than normal cells, the AIE-mito-TPP probe can selectively accumulate in cancer-cell mitochondria and light up its fluorescence. More importantly, the probe exhibits selective cytotoxicity for studied cancer cells over normal cells. The high potency of AIE-mito-TPP correlates with its strong ability to aggregate in mitochondria, which can efficiently decrease the mitochondria membrane potential and increase the level of intracellular reactive oxygen species (ROS) in cancer cells. The mitochondrial light-up probe provides a unique strategy for potential image-guided therapy of cancer cells.*

Targeted delivery of diagnostic and therapeutic agents to cancer cells with image-guided therapy is a great challenge. One of the bottlenecks is the lack of specificity, which results in systemic toxicity and a high dosage requirement.[1] To tackle this challenge, direct delivery of chemotherapy agents to subcellular organelles has gained much attention for improving therapy efficiency, minimizing side effects, and decreasing multi-drug resistance.[2] Mitochondria are vital subcellular organelles in eukaryotic cells and mitochondrial dysfunctions have been linked to multiple aspects of tumorigenesis and tumor progression.[3] Targeting mitochondria has emerged as a new strategy for improved therapeutic efficiency.

[*] Dr. Q. Hu,[+] G. Feng, Prof.Dr. B. Liu
Department of Chemical and Biomolecular Engineering
National University of Singapore
4 Engineering Drive 4, Singapore 117585 (Singapore)
E-mail: cheliub@nus.edu.sg
Dr. M. Gao,[+] Prof.Dr. B. Liu
Institute of Materials Research Engineering (A*STAR)
3 Research Link, Singapore 117602 (Singapore)
[+] These authors contributed equally to this work.

[**] We thank the Singapore National Research Foundation (R-279-000-390-281), the SMART (R279-000-378-592), Ministry of Defense (R279-000-340-232), National University of Singapore (R279-000-415-112) and the Institute of Materials Research and Engineering of Singapore Engineering (A*STAR) (IMRE/12-8P1103) for financial support.

Supporting information for this article is given via a link at the end of the document. Supporting information for this article is available on the WWW under http://dx.doi.org/10.1002/anie.201408897.

Triphenylphosphonium (TPP), a cation with lipophilicity and delocalized positive charge, can accumulate selectively within energized mitochondria because of the negative potential gradient of the organelle. This property has been applied to deliver imaging and therapeutic cargoes to mitochondria.[4] Additionally, mitochondria-targeting peptides were also reported to be successful for subcellular targeting.[5] To construct mitochondria-targeted therapy agents, the most common strategy is to conjugate a mitochondria-targeting moiety with model drugs or to load drugs into surface-functionalized nanoparticles.[6] To monitor the mitochondria-specific drug delivery using fluorescence techniques, additional conjugation of a fluorescent tag is required. Such modifications have the potential to alter the pathway of drug molecules, and the fluorescence is not correlated with the drugs once they are released. Therefore, the development of fluorescent therapeutic agents with mitochondria targeting is highly desirable to track them and directly visualize their therapeutic effects.[6b,7]

The discovery of fluorogens which can undergo aggregation-induced emission (AIE) has opened up new opportunities to develop light-up fluorescent probes for sensing and imaging.[8] AIE fluorogens generally have rotor structures, which show very weak fluorescence in dilute solutions but become highly emissive in the aggregated state.[9] To further enhance the imaging contrast and signal-to-noise ratio, fluorogens which can undergo both AIE and excited-state intramolecular proton transfer (ESIPT) have been used to develop fluorescent light-up probes.[10] As ESIPT fluorogens can induce fluorescence change through intramolecular hydrogen bonding, fluorogens with both AIE and ESIPT characteristics offer additional advantages, such as a low background signal in aqueous media with a large Stokes shift.[11] Despite the fact that several AIE probes have been developed for sub-organelle fluorescence imaging,[8a,12] to date none have shown any therapeutic effect. As many AIE probes aggregate in cells producing a fluorescence signal, we therefore hypothesize that a mitochondria-targeting AIE probe might be able to quickly accumulate in mitochondria and form fluorescent aggregates, which will induce cell stress and lead to mitochondrial dysfunction for cancer-cell killing. It has been established that cancer cells usually have more negative mitochondrial membrane potentials than normal cells, thus offering new opportunities to enrich cancer-cell mitochondria with more AIE probes for selective cancer-cell killing over normal cells.[13]

Herein, a fluorescent probe AIE-mito-TPP with both AIE- and ESIPT-emission characteristics is designed by conjugation of a salicyladazine fluorophore with the mitochondria-targeting TPP. The fluorescence of the probe can

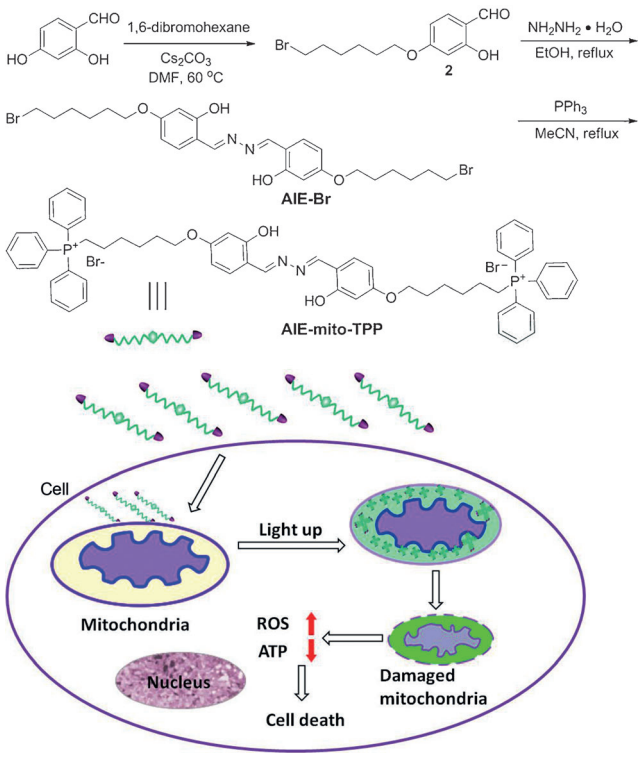

Scheme 1. Synthesis of AIE-mito-TPP and schematic representation of intracellular tracking and the therapeutic effect of AIE-mito-TPP in cancer cells. The probe crosses the cell membrane (indicated by the outer purple circle) and is taken up by the mitochondria. Within the mitochondria the probe self-aggregates to emit a fluorescence signal (as indicated by the term "light up"). The probe causes mitochondrial membrane damage and subsequently induces the generation of ROS (reactive oxygen species), inhibits ATP (adenosine triphosphate) production, and ultimately induces cancer-cell death. DMF = dimethylformamide.

only be turned on when the rotation around the N–N bond is restricted and the intramolecular hydrogen bonds are formed. The probe shows almost no fluorescence in cell-culture media but has the ability to target and switch on its fluorescence upon aggregation in mitochondria. It also exhibits higher cellular uptake, better selectivity, and much higher cytotoxicity to the cancer cell lines tested herein than to normal cell lines. We found that the predominant accumulation of the probe in cancer-cell mitochondria could indeed induce mitochondrial dysfunction, which affected several important cellular processes (Scheme 1) and led to selective cancer-cell death.

The probe was synthesized according to Scheme 1. The reaction between 2,4-dihydroxybenzaldehyde and 1,6-dibromohexane led to compound **2**, which was further reacted with hydrazine hydrate to afford AIE-Br. AIE-Br was subsequently reacted with TPP to afford the probe AIE-mito-TPP in 91% yield. The purified products were characterized by NMR spectroscopy and mass spectrometry to confirm their structures, and the experimental results are in good agreement with the theoretical values (Figure S1–S3 in the Supporting Information).

The photophysical properties of the probe are shown in Figure S4. ATP-mito-TPP shows an absorption maximum at $\lambda = 356$ nm in DMSO in the UV/Vis absorption spectrum and almost no fluorescence is detected. However, it is highly emissive in the solid state with an emission maximum at $\lambda =$ 505 nm which is due to the ESIPT and AIE effects.[9,11] There is almost no overlap between the absorption and emission spectra with a large Stokes shift of 149 nm, which is desirable for bioimaging with minimal self-absorption.

First, we compared the intracellular localization of AIE-mito-TPP in HeLa and normal fibroblast NIH-3T3 cells. Both cells were treated with the probe (1 μM) for two hours, which were co-stained with MitoTracker (a mitochondrial stain) or LysoTracker (a lysosomal stain). For HeLa cells, confocal microscopy analysis shows that the green fluorescence signal is well-overlapped with the red fluorescence signal from the MitoTracker (Figure 1 A). However, there is almost no

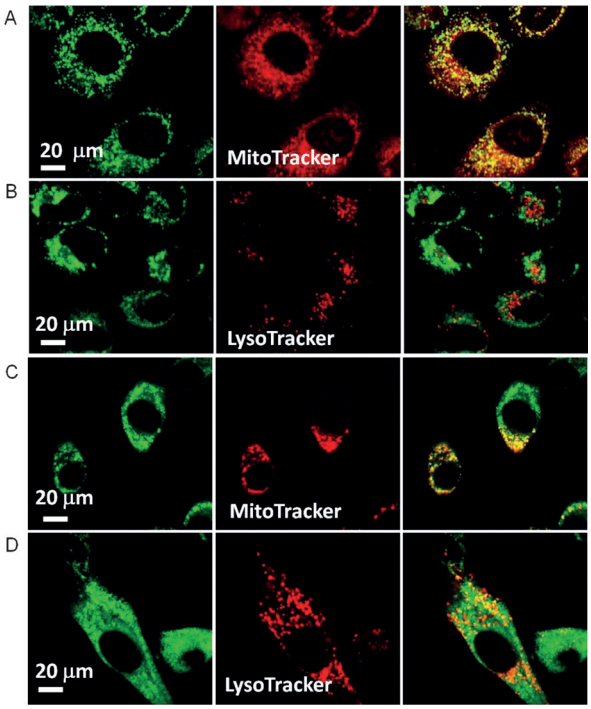

Figure 1. Confocal microscopy images of A, B) HeLa cells and C, D) NIH-3T3 cells after incubation with AIE-mito-TPP (1 μM). The cells were co-stained with A, C) MitoTracker (200 nM) or B, D) LysoTracker (100 nM). For AIE-mito-TPP, an excitation wavelength $\lambda_{ex} =$ 405 nm and a band-pass filter of $\lambda = 510$–560 nm were used. For MitoTracker and LysoTracker: $\lambda_{ex} = 543$ nm, band-pass filter $\lambda = 575$–625 nm. Scale bar for all images = 20 μm.

overlap in the fluorescence signals between the probe and LysoTracker (Figure 1 B). The Pearson correlation coefficients, used to quantify the overlap between AIE-mito-TPP emission and MitoTracker or LysoTracker emission, are calculated as 0.81 and 0.23, respectively (Figure S5A–C). For fibroblast NIH-3T3 cells, the probe is distributed in both mitochondria and lysosomes (Figures 1 C and D) and the Pearson correlation coefficients are 0.70 and 0.50, respec-

tively (Figure S5 D–F). These results demonstrate that the probe exhibits better selectivity for mitochondria in HeLa cells compared to NIH-3T3 cells.

Considering that carcinoma cells a have higher mitochondria membrane potential than normal cells,[13b] we investigated the cellular uptake of the probe in HeLa and NIH-3T3 cells. The uptake of the probe (1.0 μM) by HeLa cells is time- and concentration-dependent and increases rapidly in the first 30 minutes, followed by a slow increase over the course of the two hour study (Figure S6 A, B). A similar uptake pattern is also measured for NIH-3T3 cells (Figure S6 C, D). However, the fluorescence intensity of the probe-stained HeLa cells is twice and 1.5 times that of the NIH-3T3 cells after 0.5 and 1.0 hours incubation, respectively, revealing that the probe uptake is more efficient in HeLa cells. This phenomenon is also detected in a panel of normal and cancer cell lines (Figure S7). The selectivity is largely because of the difference in mitochondrial membrane potential between normal and cancer cells. Previous studies have shown that the approximately 60 mV potential difference between normal epithelial cells and carcinoma cells could result in a tenfold uptake difference at 37 °C.[7b,13] Additionally, the plasma membrane potential is also reported to be higher for carcinoma cells than normal epithelial cells,[13b] which also favors probe uptake for carcinoma cells. It is also found that AIE-Br (1.0 μM) can hardly enter the HeLa cells, indicating that TPP is not only a mitochondria-targeting ligand, but also favors cellular uptake (Figure S8).

We next used an MTT cell viability assay to study the cytotoxicity of AIE-Br and AIE-mito-TPP for HeLa and NIH-3T3 cells. AIE-Br shows low cell toxicity to both cell lines, in agreement with its poor cellular uptake. AIE-mito-TPP even at a low concentration (0.5–1.0 μM) exhibits high cytotoxicity to HeLa (Figure 2 A) and MDA-MB-231 cells (Figure S9) after 24 hours incubation, but it has low cytotoxicity to NIH-3T3 cells (Figure 2 B). To further corroborate these observations, we tested the anti-proliferative activities of AIE-mito-TPP in a panel of control cell lines and cancer cell lines using a CellTiter 96® aqueous one-solution cell proliferation assay. 50 % of the growth inhibition (GI_{50}) was achieved at 0.17–0.45 μM in all tested cancer cell lines, demonstrating the excellent anticancer activity of the probe (Figure S10 A and Table S1). The probe is approximately 9 to 19 times more potent in HeLa cells than in the tested control cell lines (Figure S10 B, Table S1). The difference in potency between cancer cell lines and normal cell lines indicates good selectivity for the probe.

AIE-mito-TPP was subsequently used to monitor HeLa cell death together with propidium iodide (PI), a dye that can only be taken up by dead or dying cells (Figure 2 C–H). To induce rapid cell death, HeLa cells were exposed to 2 μM of the probe. AIE-mito-TPP selectively accumulates in mitochondria and induces a fluorescence signal within one hour. This, together with the negligible background signal from the culture media, confirms the AIE character of the probe. As the incubation time increases, PI gradually enters the cells and stains the nuclei, giving rise to a red fluorescence signal. The percentage of PI-stained cells increases during the period of three to eight hours. After incubation for five hours, the cell

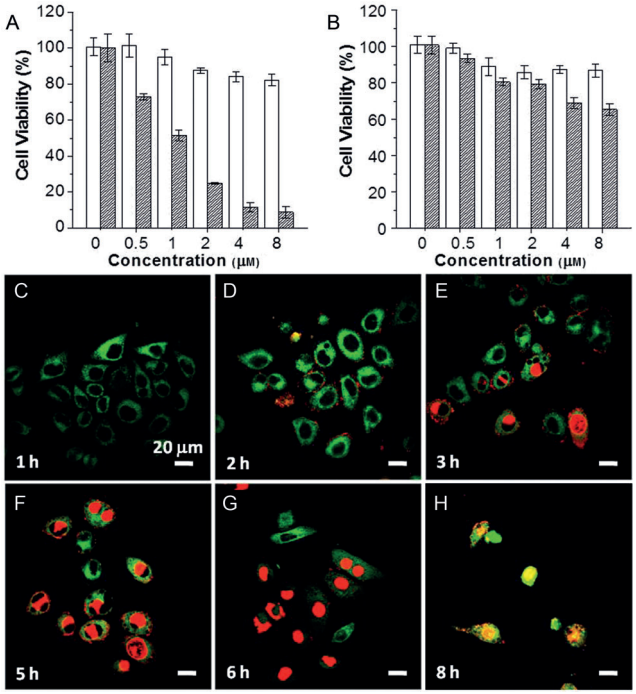

Figure 2. Cell viabilities of A) HeLa cells and B) NIH-3T3 cells after incubation with different concentrations of AIE-Br (white bars) and AIE-mito-TPP (shaded bars) for 24 hours. C)–H) Confocal microscopy images showing HeLa cell death upon incubation with AIE-mito-TPP (2 μM) for 1 hour, followed by propidium iodide (PI) stain. Images are shown at various time intervals (1h–8h). For AIE-mito-TPP: $\lambda_{ex} = 405$ nm, band-pass filter $\lambda = 510$–560 nm. For PI: $\lambda_{ex} = 543$ nm, band-pass filter $\lambda = 575$–625 nm. Scale bar for all images = 20 μm.

cytoplasm shrinks and forms large vacuoles, which are typical characteristics of cell apoptosis. When the incubation time is eight hours, the nuclear membrane is destroyed and the probe also enters the nuclei (Figure 2 H).

To assess whether the probe aggregation in mitochondria is involved in mitochondrial dysfunction, we first used tetramethylrhodamine ethyl ester (TMRE),[14] a specific mitochondrial dye with red–orange fluorescence, to detect the changes in mitochondrial membrane potential caused by AIE-mito-TPP. The PBS-treated healthy cells (PBS = phosphate buffered saline) as control show bright-red fluorescence (Figure 3 A), whereas the fluorescence from the TMRE stain is significantly decreased in HeLa cells after treatment with the probe (1 μM) for two hours (Figure 3 B). However, similar bright-red fluorescence is detected in both control and the probe treated NIH-3T3 cells (Figure 3 C and D). The confocal images reveal that the probe can selectively depolarize the mitochondrial membrane potential in HeLa cells, which is further confirmed by quantitative flow cytometry analysis. As compared to the high fluorescence intensity of the control healthy cells, the probe-treated HeLa cells show a concentration-dependent decrease in the TMRE fluorescence intensity. The probe (1 μM) is found to induce a sufficient decrease in mitochondrial membrane potential (Figure 3 E), indicating membrane damage. However, in Figure 3 F, the PBS-treated control cells and the probe treated NIH-3T3 cells show a similar bright fluorescence intensity, which suggests the integrity of the mitochondria membrane.

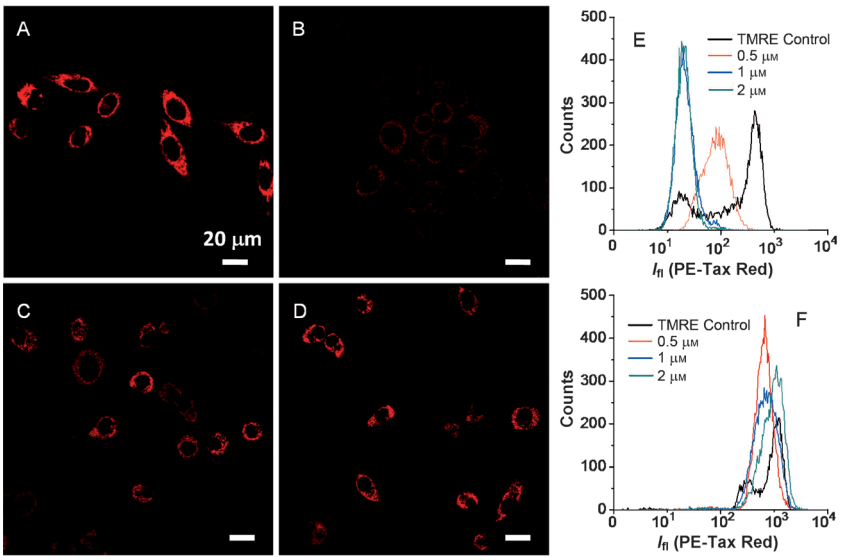

Figure 3. Confocal microscopy images showing the measurement of mitochondrial membrane potential using TMRE in A, B) HeLa and C, D) NIH-3T3 cells without (A, C) and with (B, D) AIE-mito-TPP (1 μM) treatment for 2 hours. For TMRE: $\lambda_{ex} = 543$ nm, emission was detected at $\lambda = 575$–625 nm. E, F) The quantitative analysis of TMRE fluorescence intensity in HeLa (E) and NIH-3T3 (F) cells by flow cytometry upon incubating the cells with different concentrations of AIE-mito-TPP for 2 hours. Scale bar for all images = 20 μm. I_{fl} (PE-Tax Red) = fluorescence intensity of the dye PE-Tax Red.

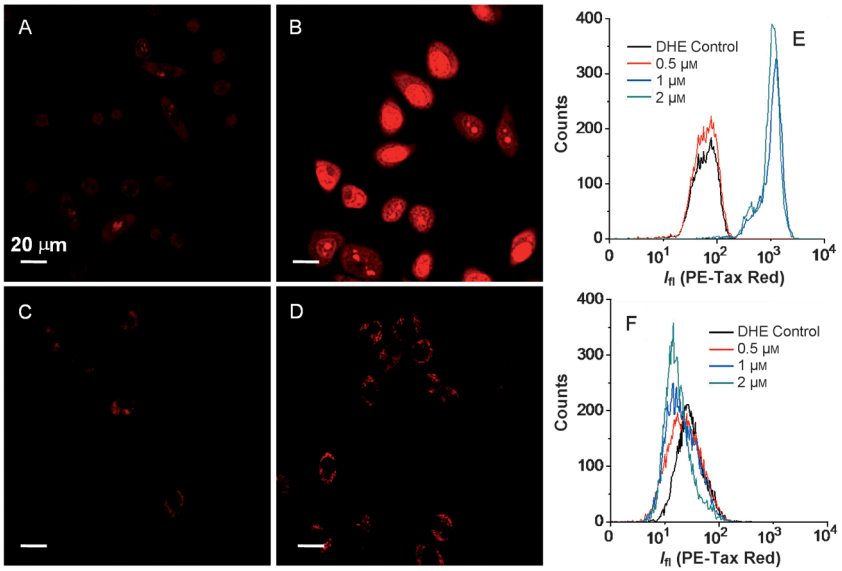

Figure 4. Confocal images showing the generation of ROS as measured by dehydroethidium (DHE) in A, B) HeLa and C, D) NIH-3T3 cells without (A, C) and with (B, D) treatment with the probe (1 μM) for 2 hours. For DHE: $\lambda_{ex} = 543$ nm, emission was detected at $\lambda = 575$–625 nm. E, F) The quantitative analysis of ROS generation in HeLa (E) and NIH-3T3 (F) cells by flow cytometry after incubating the cells with different concentrations of the probe. Scale bar for all images = 20 μm. I_{fl} (PE-Tax Red) = fluorescence intensity of the dye PE-Tax Red.

To understand cell oxidative stress caused by AIE-mito-TPP treatment, we monitored the level of intracellular reactive oxygen species (ROS) for both HeLa and NIH-3T3 cells using dehydroethidium (DHE) as an indicator. DHE can react with superoxide radicals to form 2-hydroxyethidium, which intercalates with DNA to yield bright fluorescence. The brightness of the red fluorescence in cell nuclei is thus correlated with ROS generation. As shown in Figure 4 A–D, upon incubation of HeLa cells and NIH-3T3 cells with the probe (1 μM) for two hours, only HeLa cells show bright red fluorescence, whereas that for NIH-3T3 cells remains low, indicating high ROS generation in HeLa cells. Quantitative measurement of ROS generation was conducted by flow cytometry, which shows that 1 μM of the probe is sufficient to maximize ROS generation (Figure 4 E) for HeLa cells, but not for NIH-3T3 cells (Figure 4 F). As the probe itself in solution does not produce obvious ROS, this is the first report that an AIE probe is able to induce significant ROS generation in cancer cells over normal cells in the absence of light illumination. Cancer cells are often under increased oxidative stress as compared to normal cells, thus further increasing the level of ROS can selectively cause greater damage to cancer cells.[15]

Mitochondria are the powerhouses of cells and serve as the major energy source to maintain the cancer-cell proliferation, invasion, and metastasis.[16] It is postulated that mitochondria dysfunction in cancer cells would affect the relative cellular ATP production and cell cycle, apoptosis, and migration processes. The relative ATP activity in HeLa cells decreases progressively with the increased amount of probe used for cell incubation. As compared with PBS-treated cells, the relative intracellular ATP activity in HeLa cells treated with 1.0 and 2.0 μM of the probe decreased to 50% and 25% of the control, respectively.

The effects of the probe on HeLa cell-cycle kinetics, cell apoptosis, and migration were subsequently investigated, using untreated cells as the control. After 24 hours incubation, for HeLa cells treated with the probe (1 μM), the percentage of cells in the G_0/G_1 phase ($73.9 \pm 1.9\%$) is more than that of the control ($63.4 \pm 2.9\%$). The decrease of the proliferative index for AIE-mito-TPP treated cells indicates that the probe inhibits the growth of the HeLa cells by arresting their cell cycle progression in the G_0/G_1 phase (Figure S11 A–C). The apoptotic ability of the probe on HeLa cells was also studied by TUNEL staining, which detects DNA fragmentation (TUNEL = terminal deoxynucleotidyl transferase-mediated dUTP nick end labeling). As shown in Figure S11 D, treatment of HeLa cells with a higher concentration of AIE-mito-TPP yields a higher percentage of

TUNEL-positive cells, indicative of obvious cell apoptosis. To further understand whether the probe treatment affects the migration of HeLa cells, a cell-scratch spatula was applied to make a scratch in the cell monolayer, and the phase contrast images of HeLa cells were taken before and after incubation with the probe for 48 hours. As shown in Figure S12 A and S12 D, after 48 hours incubation the PBS-treated control cells migrate into the wound area. However, the wound closure in the probe-treated HeLa cells is inhibited (Figure S12 B, C, E, and F). The HeLa cell migration ratios exposed to the probe at concentrations 0.5 and 1.0 μM are 60% and 19%, respectively, compared to the PBS-treated cells. As cancer cells are highly invasive with metastatic properties,[17] the inhibition of their migration should also contribute to effective cancer treatment. Collectively, our results validate that the aggregation of AIE-mito-TPP probes in mitochondria is responsible for their cytotoxicity and suggest that their preferential aggregation within cancer-cell mitochondria makes them a potential agent for cancer-cell imaging and therapy. However, several issues, such as pharmakokinetics, systemic toxicity in animals, and systemic localization, await further investigation before the probe could be used for real cancer therapy.

In conclusion, we developed a mitochondria-targeted light-up probe AIE-mito-TPP and reported its selective anticancer activity. The probe is almost nonfluorescent in culture medium, and is able to quickly and selectively accumulate in and light-up mitochondria in cancer cells over normal cells. The probe accumulation in cancer-cell mitochondria was found to decrease the mitochondrial membrane potential, induce the generation of ROS, inhibit ATP production, and affect essential cancer-cell progress. The AIE-based strategy provides a new platform for organelle-targeted imaging and treatment. In light of the imaging and anticancer performance of this probe, the further design of AIE-based probes with red and near-infrared emission will open new opportunities for the development of potential therapeutic agents for in vivo diagnosis and therapy.

Received: September 8, 2014
Published online: October 15, 2014

Keywords: aggregation-induced emission · bioimaging · cancer cells · imaging agents · mitochondria

[1] a) C. F. Meares, A. J. Chmura, M. S. Orton, T. M. Corneillie, P. A. Whetstone, *J. Mol. Recognit.* **2003**, *16*, 255 – 259; b) C. Holohan, S. Van Schaeybroeck, D. B. Longley, P. G. Johnston, *Nat. Rev. Cancer* **2013**, *13*, 714 – 726.

[2] a) L. Rajendran, H. J. Knolker, K. Simons, *Nat. Rev. Drug Discovery* **2010**, *9*, 29 – 42; b) N. M. Sakhrani, H. Padh, *Drug Des. Dev. Ther.* **2013**, *7*, 585 – 599.

[3] a) D. Trachootham, J. Alexandre, P. Huang, *Nat. Rev. Drug Discovery* **2009**, *8*, 579 – 591; b) V. Gogvadze, *Curr. Pharm. Des.* **2011**, *17*, 4034 – 4046.

[4] a) B. C. Dickinson, C. J. Chang, *J. Am. Chem. Soc.* **2008**, *130*, 9638 – 9639; b) W. Chyan, D. Y. Zhang, S. J. Lippard, R. J. Radford, *Proc. Natl. Acad. Sci. USA* **2014**, *111*, 143 – 148; c) J. Wang, C. T. Yang, Y. S. Kim, S. G. Sreerama, Q. Cao, Z. B. Li, Z. He, X. Chen, S. Liu, *J. Med. Chem.* **2007**, *50*, 5057 – 5069; d) R. A. Smith, C. M. Porteous, A. M. Gane, M. P. Murphy, *Proc. Natl. Acad. Sci. USA* **2003**, *100*, 5407 – 5412.

[5] a) R. Mourtada, S. B. Fonseca, S. P. Wisnovsky, M. P. Pereira, X. Wang, R. Hurren, J. Parfitt, L. Larsen, R. A. Smith, M. P. Murphy, A. D. Schimmer, S. O. Kelley, *PloS one* **2013**, *8*, e60253; b) L. M. Wittenhagen, J. R. Carreon, E. G. Prestwich, S. O. Kelley, *Angew. Chem. Int. Ed.* **2005**, *44*, 2542 – 2546; *Angew. Chem.* **2005**, *117*, 2598 – 2602; c) S. O. Kelley, K. M. Stewart, R. Mourtada, *Pharm. Res.* **2011**, *28*, 2808 – 2819.

[6] a) M. Millard, J. D. Gallagher, B. Z. Olenyuk, N. Neamati, *J. Med. Chem.* **2013**, *56*, 9170 – 9179; b) S. Marrache, S. Dhar, *Proc. Natl. Acad. Sci. USA* **2012**, *109*, 16288 – 16293; c) S. Biswas, N. S. Dodwadkar, P. P. Deshpande, V. P. Torchilin, *J. Controlled Release* **2012**, *159*, 393 – 402.

[7] a) M. Millard, D. Pathania, Y. Shabaik, L. Taheri, J. Deng, N. Neamati, *PloS one* **2010**, *5*, e13131; b) Y. H. Shabaik, M. Millard, N. Neamati, *PloS one* **2013**, *8*, e54346.

[8] a) C. Li, T. Wu, C. Hong, G. Zhang, S. Liu, *Angew. Chem. Int. Ed.* **2012**, *51*, 455 – 459; *Angew. Chem.* **2012**, *124*, 470 – 474; b) D. Ding, K. Li, B. Liu, B. Z. Tang, *Acc. Chem. Res.* **2013**, *46*, 2441 – 2453; c) Y. Huang, F. Hu, R. Zhao, G. Zhang, H. Yang, D. Zhang, *Chem. Eur. J.* **2014**, *20*, 158 – 164; d) K. Li, B. Liu, *Chem. Soc. Rev.* **2014**, *43*, 6570 – 6597; e) T. Noguchi, A. Dawn, D. Yoshihara, Y. Tsuchiya, T. Yamamoto, S. Shinkai, *Macromol. Rapid Commun.* **2013**, *34*, 779 – 784; f) X. Li, K. Ma, S. Zhu, S. Yao, Z. Liu, B. Xu, B. Yang, W. Tian, *Anal. Chem.* **2014**, *86*, 298 – 303; g) J. Zhao, D. Yang, Y. Zhao, X. J. Yang, Y. Y. Wang, B. Wu, *Angew. Chem. Int. Ed.* **2014**, *53*, 6632 – 6636; *Angew. Chem.* **2014**, *126*, 6750 – 6754.

[9] a) Y. Hong, J. W. Lam, B. Z. Tang, *Chem. Soc. Rev.* **2011**, *40*, 5361 – 5388; b) Z. Chi, X. Zhang, B. Xu, X. Zhou, C. Ma, Y. Zhang, S. Liu, J. Xu, *Chem. Soc. Rev.* **2012**, *41*, 3878 – 3896.

[10] a) M. Gao, C. K. Sim, C. W. Leung, Q. Hu, G. Feng, F. Xu, B. Z. Tang, B. Liu, *Chem. Commun.* **2014**, *50*, 8312 – 8315; b) M. Gao, Q. Hu, G. Feng, B. Tang, B. Liu, *J. Mater. Chem. B* **2014**, *2*, 3438 – 3442.

[11] J. Wu, W. Liu, J. Ge, H. Zhang, P. Wang, *Chem. Soc. Rev.* **2011**, *40*, 3483 – 3495.

[12] C. W. Leung, Y. Hong, S. Chen, E. Zhao, J. W. Lam, B. Z. Tang, *J. Am. Chem. Soc.* **2013**, *135*, 62 – 65.

[13] a) M. P. Murphy, R. A. Smith, *Annu. Rev. Pharmacol. Toxicol.* **2007**, *47*, 629 – 656; b) L. B. Chen, *Annu. Rev. Cell Biol.* **1988**, *4*, 155 – 181; c) J. S. Modica-Napolitano, J. R. Aprille, *Adv. Drug Delivery Rev.* **2001**, *49*, 63 – 70.

[14] B. Chazotte, *Cold Spring Harbor Protoc.* **2011**, *2011*, 895 – 897.

[15] X. Wang, S. Peralta, C. T. Moraes, *Adv. Cancer Res.* **2013**, *119*, 127 – 160.

[16] R. Scatena, *Adv. Exp. Med. Biol.* **2012**, *942*, 329 – 346.

[17] W. H. Clark, *Br. J. Cancer* **1991**, *64*, 631 – 644.

